

Simulations of ITER Disruption and VDE scenarios with TSC and comparison with DINA results

I. Bandyopadhyay 1), Y. Nakamura 2), M. Sugihara 3), H. Fujieda 2), A. Sen 1), S.C. Jardin 4)

1) ITER-India, Institute for Plasma Research, Bhat, Gandhinagar, India

2) Japan Atomic Energy Agency, Naka-shi, Ibaraki-ken, Japan

3) ITER International Team, ITER, CEA-Cadarache, France

4) Princeton Plasma Physics Laboratory, Princeton, New Jersey, USA

e-mail: indranil@ipr.res.in

Abstract. Vertical Displacement Events (VDEs) and plasma current disruptions can seriously degrade the lifetime of in-vessel components in ITER, as large electromagnetic and thermal loads can be induced at such events. Hence, accurate modelling of such events is crucial for estimating disruption induced forces. In the past, ITER disruption modelling has been carried out using the DINA code. However, since predictive simulation of such events depend on a large number of model assumptions, the resultant predictions may contain significant error bars. It is important therefore to validate the code results with other models. With such an objective in mind, we have carried out VDE and Disruption simulations using the Tokamak Simulation Code (TSC) and the results are compared with the earlier DINA predictions. The two model predictions match reasonably well, especially in the early linear part of the vertical evolution, though there are some differences in the phase dominated by halo currents.

1. Introduction

Vertical Displacement Events (VDEs) and plasma current disruptions, that can induce large electromagnetic and thermal loads, constitute a major concern for the lifetime of in-vessel components in ITER, as well as for machine robustness. Accurate modelling of such events is therefore crucial for a proper estimation of these induced forces. The present estimates for such forces on ITER are largely based on modelling studies [1] carried out using the DINA code [2]. However, the principal physical outputs of these simulations such as the plasma current quench time, the vertical position evolution, the drop in internal inductance etc., may be significantly influenced by model assumptions and model dependent input parameters of a given code and consequently affect the derivation of load specifications. Furthermore the electromagnetic properties of the machine play an important role in determining the plasma dynamics and thus extrapolations for ITER based on present day machines may have significant uncertainties. Hence, it is important to validate and benchmark the results against similar simulations carried out on another independent code. While reviewing the design specifications for VDEs and major disruptions during the 2007 design review, it was recommended that further validation of the specifications through additional simulations using the Tokamak Simulation Code (TSC) [3] was desirable. The TSC code was particularly recommended as it has been very successful in the past in reproducing experimental VDE and disruption data of several present day tokamaks [4-7]. However it should be added that predictive modelling of disruption and VDE scenarios in ITER is a more complex task compared to the interpretative modelling of existing tokamak discharges that has been done in the past. This is because, in interpretative modelling one has the experimental data available, some of which are used to fine-tune the inputs to the codes to make the model predictions closely match the experiments. For example, halo width and temperature, post disruption plasma temperature etc which are critical for getting good experimental validation, have significant uncertainties in predictive modelling. Hence the present simulations

are aimed at primarily defining an error bar on the estimates of the predictions by DINA of the halo currents and forces arising during these events.

In this paper we present the simulation results for major disruptions (MD) and VDEs in ITER using the TSC code and its comparison with the earlier DINA results. In all these simulations, the initial plasma is taken according to ITER operational scenario 2 end-of-burn (EOB) specifications (15 MA) [8]. Some of the critical plasma parameters used in these simulations are given in Table 1. For the MD simulations, the plasma current quench is triggered by a beta quench simulated by dropping the central electron temperature artificially (no transport is calculated) from an initial $\langle T_e \rangle = 8.8$ keV to 6.0 eV in a time of 1 msec. In the VDE simulations, the vertical position control is switched off and the plasma is allowed to move vertically till the edge safety factor (q_{95}) reaches a value of 1.5. At that point the beta crash is initiated in the same way as in the MD case, with the difference that while the post crash temperature is kept at 6 eV for the fast current quench it is kept at 50 eV for the slow current quench.

Table 1: Some critical plasma parameters used during Major Disruptions and VDEs

	Major disruptions	VDEs
Thermal Quench (TQ) phase		
TQ onset condition	Specified time	Specified edge q
Beta drop at TQ	0.7	←
Time duration of beta drop	1msec	←
Time duration for current flattening	100 μ sec	←
Change of l_i	~ 0.2	←
Time duration of helicity recovery	2msec	←
Current Quench (CQ) phase		
Electron temperature (including halo region)	Fixed to 6eV during CQ	Fixed to 6eV during CQ for fast CQ Fixed to 50eV during CQ for slow CQ
Z_{eff} (including halo region)	Fixed to 2 during CQ	←

In section 2, we highlight some of the important differences between the DINA and the TSC models that can potentially impact on the simulation results. The details of the simulation results are given in section 3 and the conclusions summarised in section 4.

2. Model differences

There are some significant differences in the model assumptions of the two codes whose influence on the final results need to be ascertained. For example, one of the major differences in the two models is in the treatment of the halo current dynamics, which probably plays the most crucial role in the load calculation. In both the models, for disruption as well as for the VDE simulations, the plasma column is allowed to move vertically till it becomes limited as it touches the first wall (FW). At this point the halo current model is switched on, with a halo temperature constant at 6 eV. In the DINA model, the width of the halo region is calculated using semi-

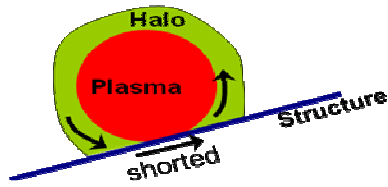


Figure 1: Schematic of halo path as treated in DINA

resistance). In TSC, conductors within the computational domain are treated as toroidal current carrying filaments with cross-sections equal to the grid size. To treat toroidally discontinuous

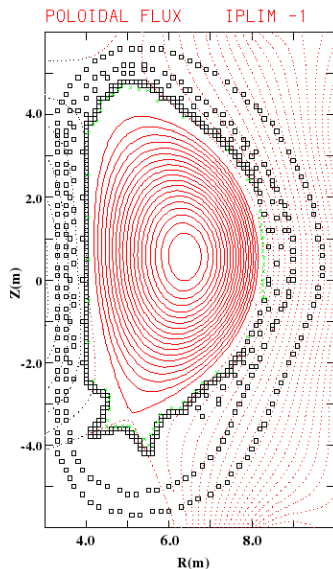


Figure 2: Initial plasma equilibrium and the vessel/FW as modelled in TSC.

empirical analytic formula calibrated with JT-60U experiments, whereas it is set equal to 10% of the closed flux surface width in TSC. In DINA, the detailed halo current dynamics in the FW is not taken into account. Instead the halo current path between the two locations where the plasma touches the FW (Figure 1) is short circuited. Thus the poloidal halo current which flows through the halo region of the plasma, gets in and out of the conductor at the two ends where the plasma touches the FW, passing through a specified resistance path (usually zero

resistance). In TSC, conductors within the computational domain are treated as toroidal current carrying filaments with cross-sections equal to the grid size. To treat toroidally discontinuous structures, e.g. the blanket modules in ITER, one can specify a large ‘gap’ resistance in these filaments to ensure that no toroidal currents flow through them. However if there is a poloidal current path existing between adjacent conductor filaments, then a poloidal current can flow with the resistance of the conducting path as defined by the connected contour of the filament centres and their resistivity. The inductance for this poloidal current path is determined by the geometry of the conducting structure assuming axisymmetry. Thus any important effects arising from the resistance and inductance of the poloidal halo current in the passive structures can be assessed more realistically in TSC simulations. Figure 2 illustrates the TSC model of the electromagnetic structure of ITER and the initial plasma equilibrium configuration. In the TSC description, to simulate the DINA model as closely as possible, a poloidally semi-continuous current path with very low resistance is provided through the FW in the top and bottom region against which the plasma leans during a vertical displacement. Note that, in practice the FW in ITER consists of the blanket modules which are poloidally discontinuous, but may nevertheless have a poloidal current path through the blanket supports and vacuum vessel. This model can be further improved in future to define more detailed poloidal current paths from FW to vessel through the support structures and back into the FW and finally to the plasma.

This can provide the detailed poloidal halo current distribution in the various FW support and vessel sectors, through which the halo currents can flow. Knowledge of such a distribution can help us arrive at more realistic estimates of the VDE and disruption halo induced forces and stresses on various ITER in-vessel components.

Another important model aspect which can influence the simulation results, especially the drop in the internal inductance, is the amount of current peaking and profile flattening immediately following the thermal quench. In DINA, this phenomenon is treated by introducing a helicity injection. In TSC, this is treated by using the “hyper-resistivity” model first introduced by Boozer [9], which is basically a phenomenological modelling of inherent three-dimensional turbulence effects into the two dimensional axi-symmetric model of TSC. In this model, the electric field in the plasma is expressed as:

$$\mathbf{E} + \mathbf{v} \times \mathbf{B} = \eta \mathbf{j} - \frac{\mathbf{B}}{B^2} \nabla \cdot \left(\lambda \frac{\nabla j_{||}}{B} \right)$$

where λ is the hyper-resistivity term. In the TSC simulations, the hyper resistivity term is switched on immediately after the beta crash, since the Boozer model is valid for low beta plasmas. The value of λ is adjusted till one gets a good match of the amount of the current peaking as obtained with DINA.

3. Comparison of the modelling results

3.1 Disruption Simulations

While modelling major disruption, the TSC simulations are started at the 6 millisecond point of the DINA simulations, as all plasma parameters prior to that are assumed stationary. The initial plasma equilibrium is formed as specified by ITER inductive scenario 2 EOB case and then the shape and position control are switched off. Before the crash both DINA and TSC start off with a centrally peaked temperature profile with $\langle T_e \rangle = 8.8 \text{keV}$ (exact profile shapes used in the two models may have some differences), which is brought down in 1 millisecond to 6eV and is kept flat after the crash in both the models. Immediately after the beta crash, the plasma undergoes a

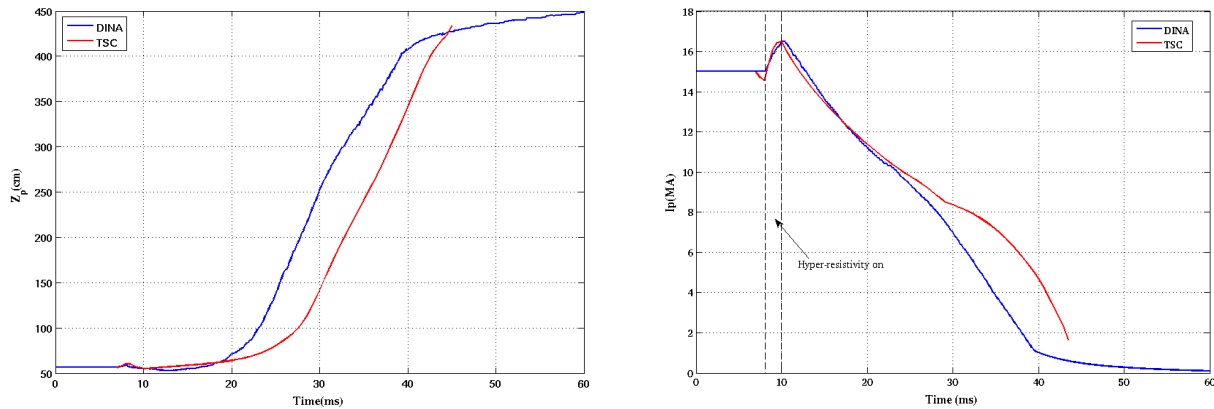


Figure 3: Plasma current and (right) plasma vertical position evolution in DINA (blue) and TSC (red) simulations

current profile flattening resulting in a drop of the internal inductance l_i . Figure 3 shows a comparison of the evolution of the plasma vertical position and current quench in the TSC and

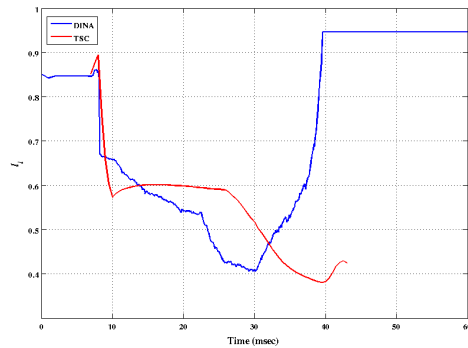


Figure 4: Internal inductance $l_i(3)$ evolution in TSC and DINA models.

DINA simulations. The vertical position grows exponentially till about 100 cms, though slower in TSC than in DINA, beyond which it grows more or less linearly in both the models. The plasma current quench in the two models also agree reasonably well, especially in the initial part of the evolution till about 20 milliseconds, including the initial current peaking immediately following the thermal quench. In TSC, the hyper-resistivity model is applied for 2 milliseconds immediately following the thermal quench, during which the plasma current rises to about 16.3MA, nearly same as that obtained using the helicity injection model of DINA. After the initial

peaking, the plasma current initially decays in both the models in approximately an exponential manner with a time constant of about 30 milliseconds. However, the evolution of the plasma current profile is somewhat different in the two models as shown in the internal inductance ($l_i(3)$) evolution in figure 4. In TSC, along with the thermal quench, there is a more pronounced initial short profile peaking. Thereafter, during the current (amplitude) peaking, the amount of profile flattening in TSC is somewhat more than that in DINA. After the thermal quench, l_i drops from about 0.85 to 0.57 in TSC which is somewhat larger than that in DINA (after the drop $l_i \sim 0.67$ in DINA). This difference could be reduced by adjusting the hyper-resistivity parameter in TSC, but that causes a reduced peaking in the current amplitude. In DINA, after the initial fast drop, l_i continues to drop at a slower rate till it reaches a value of about 0.4 at around 30 milliseconds and then starts increasing again. In TSC, on the other hand, after the initial flattening, the profile remains more or less stationary for some time before it falls again and only in the terminal stages of the disruption does it show signs of peaking. This difference in the current profile evolution is not very well understood at present and may have its origin in the difference of the halo current treatment in the two models.

Also as seen in Figure 3, beyond 20 milliseconds DINA shows a much faster (more or less linear) plasma current decay up to about 40 milliseconds, whereas in TSC simulations the exponential current quench continues till about 30 milliseconds and only thereafter shows a faster final current termination.

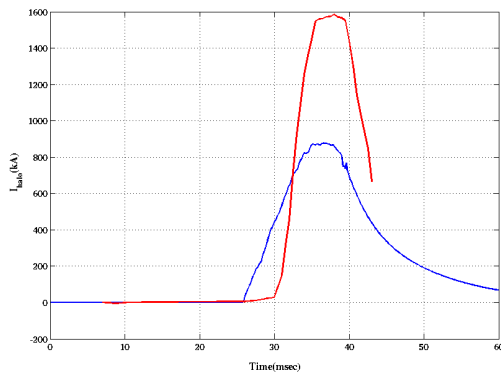


Figure 5: Evolution of poloidal halo current in TSC (red) and DINA (blue).

about 870kA in DINA with the rise and decay of the halo current being significantly faster in TSC. The halo current amplitude in TSC is about 1.8 times higher, which within the limitations inherent in the assumptions of the two models, is indicative of the uncertainties in the prediction of vessel forces in ITER and the error bar.

3.2 VDE Simulations

For the VDE scenarios in ITER, both the upward (UW) and downward (DW) VDEs have been modelled in which the plasma column is initially displaced vertically about 20 cms up or down respectively from the nominal vertical position. The vertical position control is then switched off, all PF coil currents are kept constant and the plasma column is allowed to move vertically till it becomes limited and starts shrinking. As it has been predicted [10] that in ITER VDE scenarios, the final thermal quench would happen when the edge safety factor reaches a value of $q_{95} \sim 1.5$, the same is simulated in both the TSC and DINA models by dropping the plasma temperature from $\langle T_e \rangle = 8.8 \text{ keV}$ to 6eV in fast current termination (or 50 keV in slow current termination

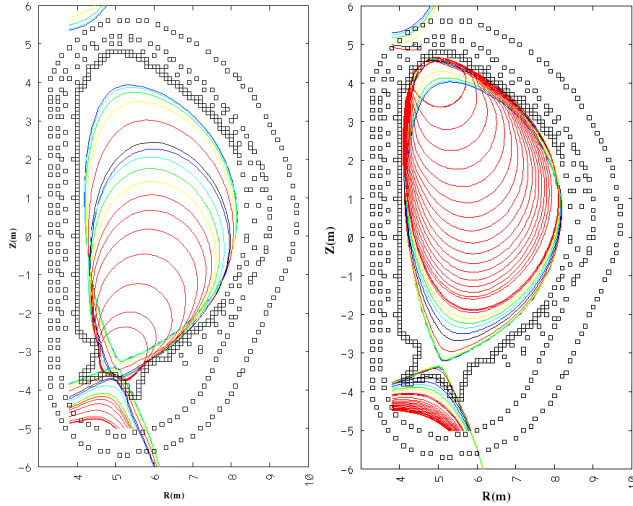


Figure 6: Evolution of the plasma separatrix in the UW and DW VDE cases.

scenario). Figure 6 shows the evolution of the plasma separatrix in the DW and UW VDE cases. In general, there is good agreement between the models in simulating the VDE scenarios, especially in the early part of the vertical evolution, highlighted in the plasma vertical position and safety factor plots shown in Figure 7. In the UW VDE case for example, the plasma become limited from about 600 milliseconds till which time the safety factor increases almost identically in both the models from about 2.9 to about 3.3, thereafter decreasing rapidly as the limited plasma starts shrinking. In TSC it takes about 19 milliseconds more than in DINA

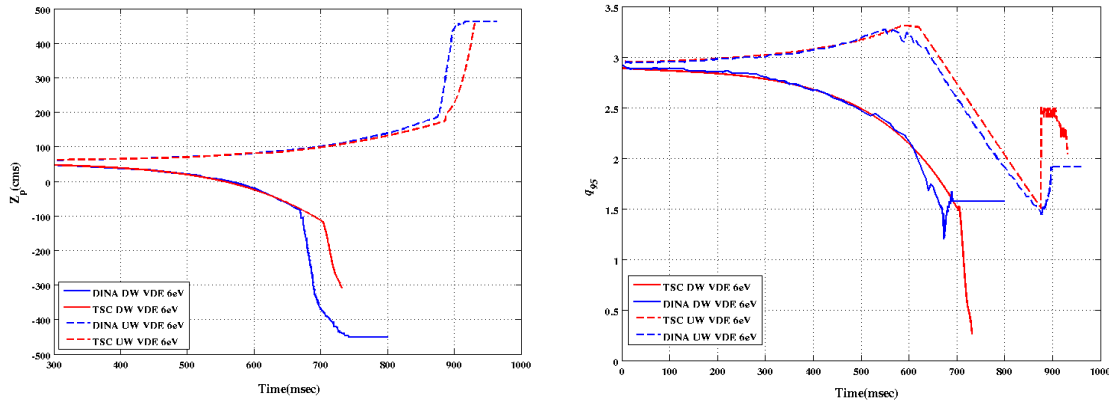


Figure 7: Vertical plasma position and safety factor (q_{95}) evolution in the DW (solid) and UW (dashed) VDE cases.

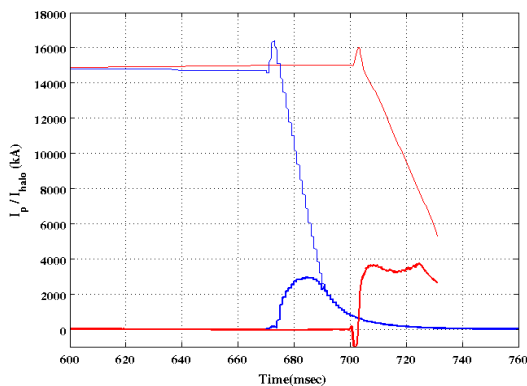


Figure 8: Plasma current (thin curves) and halo current (thick curves) evolution in DW VDE case.

for q_{95} to reach 1.5 when the beta collapse is initiated. In the final disrupting phase, the plasma vertical motion in TSC is slightly slower than in DINA, analogous to the MD case. This can be attributed to the fact that during this phase large halo currents start flowing and the differences in the halo current model is possibly responsible for this. In the DW VDE case also, there is very good agreement in the Z_p and q_{95} evolution in the two models, though q_{95} decays more or less monotonically in both diverted and limited phase of the evolution. In TSC, the plasma column moves further by about 15 cms thereby taking about 33 milliseconds more time before q_{95} reaches 1.5. In DINA, it takes about 40 milliseconds for q_{95} to go

from 2 to 1.5, whereas it takes about 70 milliseconds in TSC for the same. Figure 8 shows the evolution of the plasma and halo currents in the DW VDE case, the UW case also shows similar behaviour. The current peaking in TSC is slightly smaller than in DINA (16 MA as against 16.4 MA) which is similar as in MD simulations and is due to the difference in modelling of the profile flattening. The peak halo current magnitude in TSC in the DW VDE case is about 3.6MA, about 20% higher than in DINA (3.0MA). In the UW VDE case TSC shows a peak halo current of about 1.5MA as against 1.1 MA in DINA. However, in both the cases the duration of the halo current near its peak is larger in TSC (~ 27 ms), which is about 60% more than in DINA (16ms).

4. Conclusions

To summarise the results, simulations of major disruptions and VDEs for reference scenario 2 EOB has been carried out using TSC for validating the earlier simulations carried out in DINA. Considering the differences in the two models, the results match reasonably well for both the MD and VDE simulations, especially in the early linear part of the plasma evolution. In the MD case, the simulations match in the current quench rate for the early part of the disruption, but differences exist thereafter in the halo current phase in which the plasma quench in TSC is somewhat slower. The amplitude of the halo current shown in TSC simulation is between 20-80% higher in the MD and VDE cases. Also the duration of the halo current in the VDE case is about 60% more. This difference highlights the difficulty in predictive modelling of the disruption and VDE scenarios for ITER and is indicative of the error bar that one needs to put for the force predictions. Also we would like to point out that the model simulations presented here are a somewhat simplistic representation of the actual scenario that is likely to occur in ITER. For example, the halo current path through the FW is short circuited in DINA and to model this in TSC, the conductor resistance has been kept close to zero. Whereas this simplification may not have much of an impact on the plasma quench dynamics and the overall halo current magnitude, it is important to know the detailed halo current distribution in the FW in order to ascertain the force distribution in various FW components. In practice the FW in ITER consist of the blanket modules which are poloidally discontinuous, but connected to the vessel through electrically conducting supports. Thus, to model the detailed halo current distribution more accurately through the FW, support structure and vessel, one needs to put a more detailed electromagnetic model in TSC. Moreover, the plasma current decay would also depend strongly on the post disruption plasma temperature. In both DINA and TSC models, the plasma temperature prior to disruption is kept constant at $\langle T_e = 8.8 \text{keV} \rangle$ and the post disruption temperature is kept constant at 6 eV. However, as the plasma column slowly evolves vertically in about 700-800 milliseconds in the UW or DW VDE cases, the plasma temperature would gradually decrease, especially once the plasma becomes limited. Also the post disruption temperature would be largely decided through impurity transport as well as Joule heating, which has been ignored in the present modelling. Thus accurate current quench rate could be obtained by simultaneous self-consistent calculation of appropriate transport in the disrupting plasma.

** This report was prepared as an account of work by or for the ITER Organization. The Members of the Organization are the People's Republic of China, the European Atomic Energy Community, the Republic of India, Japan, the Republic of Korea, the Russian Federation, and the United States of America. The views and opinions expressed herein do not necessarily reflect those of the Members or any agency thereof. Dissemination of the information in this paper is governed by the applicable terms of the ITER Joint Implementation Agreement.

References:

- [1] M. Sugihara, M. Shimada, H. Fujieda, Yu. Gribov, K. Ioki, Y. Kawano, R. Khayrutdinov, V. Lukash, and J. Ohmori 2007 *Nucl. Fusion* **47**, 337.
- [2] R. Khayrutdinov and V. Lukash 1993 *J. Comput. Phys.* **109**, 193.
- [3] S.C. Jardin, N. Pomphery and J. Delucia 1986 *J. Comput. Phys.* **66**, 481.
- [4] R.O. Sayer, Y.-K.M. Peng, S.C. Jardin, A.G. Kellman and J.C. Wesley 1993 *Nucl. Fusion* **33**, 969.
- [5] Pautasso G et al 1993 Experimental investigation and modeling of Vertical Displacement Events in ASDEX Upgrade, *Proc. 20th EPS Conference on Cont. Fusion and Plasma Phys. (Lisboa)* Vol. 17, P-I-199.
- [6] Y. Nakamura, G. Pautasso, O. Gruber and S.C. Jardin 2002 *Nucl. Fusion* **44**, 1471
- [7] Y. Nakamura, R. Yoshino, N. Pomphrey and S.C. Jardin, 1996 *J. Nucl. Science and Tech.* **33**, 609.
- [8] T. Hender et al, 2007 *Nucl. Fusion* **47**, S128.
- [9] A.H. Boozer, 1986 *Plasma Physics* **35**, 133.
- [10] M. Sugihara, V. Lukash, R. Khayrutdinov and Y. Neyatani, 2004 *Plasma Phys. Control. Fusion* **46**, 1581.